

See discussions, stats, and author profiles for this publication at: <https://www.researchgate.net/publication/43512671>

Control of Charge Transport in Iridium(III) Complex-Cored Carbazole Dendrimers by Generation and Structural Modification

ARTICLE *in* ADVANCED FUNCTIONAL MATERIALS · JANUARY 2009

Impact Factor: 11.81 · DOI: 10.1002/adfm.200801144 · Source: OAI

CITATIONS

29

READS

33

5 AUTHORS, INCLUDING:



Salvatore Gambino

Università del Salento

26 PUBLICATIONS 195 CITATIONS

SEE PROFILE



Ifor David William Samuel

University of St Andrews

447 PUBLICATIONS 11,332 CITATIONS

SEE PROFILE

Control of Charge Transport in Iridium(III) Complex-Cored Carbazole Dendrimers by Generation and Structural Modification

By Salvatore Gambino, Stuart G. Stevenson, Kevin A. Knights, Paul L. Burn, and Ifor D. W. Samuel*

Here, the charge transporting properties of a family of highly phosphorescent iridium(III) complex-cored carbazole dendrimers designed to have improved charge transport by incorporating carbazole units into the dendrons are studied. Firstly, the effect of the dendrimer generation and the role of dendron for materials with one dendron per ligand of the core are considered. It is shown, in contrast to previously reported light-emitting dendrimers, that in this case the carbazolyl-based dendrons have an active role in charge transport. Next, the effect on the charge transport of attaching two dendrons per ligand to the dendrimer core is explored. In this latter case, for the so called “double dendron” material a highly non-dispersive charge transport behavior is observed, together with a time-of-flight mobility of the order of $10^{-3} \text{ cm}^2 \text{ V}^{-1} \text{ s}^{-1}$. Furthermore the lowest energetic disorder parameter (σ) ever reported for a solution-processed conjugated organic material is found, $\sigma < 20 \text{ meV}$.

1. Introduction

There is currently great interest in the development of solution-processable organic semiconductors for electronic and optoelectronic applications.^[1–6] Charge transport in organic semiconductors is a particularly important issue as it plays a key role in the operation of devices such as organic light-emitting diodes (OLEDs), solar cells, and organic field effect transistors (OFETs). In fact organic semiconductors often have dual functions, for example, charge transport and light emission in OLEDs and charge carrier

photo-generation and transport in solar cells. Since the properties of charge-transporting materials used in OLEDs, solar cells, and OFETs greatly affect the device performance, the design and synthesis of high-performance, charge transporting materials is of great importance for the development of high performance devices.

Charge transporting materials with different morphologies have been used depending upon the kind of devices. Generally, organic crystalline materials exhibit larger charge carrier mobilities than those of organic amorphous materials. Devices using organic single crystals, for example, OFETs have been reported,^[7,8] however single-crystal growth on a large area substrate for device applications is not easy. Polycrystalline materials have been

used, mostly in OFETs and organic photovoltaic devices. The grain size, grain boundaries, and molecular orientations affect the device performance.^[9]

Amorphous materials have advantages over crystalline materials in device fabrication because of their good processability, isotropic and homogenous properties. Furthermore, they generally have weaker intermolecular π – π interactions leading to higher solid state luminescence quantum efficiency. Among amorphous materials, both polymers and low-molecular weight materials have been extensively used as charge-transporting materials in devices described above. Usually, high vacuum thermal deposition and spin-coating methods are used for small molecules and polymers, respectively, for thin film deposition. It has been recognized that solution-processable materials offer a better ease of processing compared to vacuum deposited ones, but generally have lower carrier mobility. The lower mobility is generally attributed to the lower structural order that reduces intermolecular π -orbital overlap.

In the last decade several attempts have been made in order to improve carrier mobility by the realization of less disordered soluble materials. For instance, high field-effect transistor mobilities of 0.1 – $0.6 \text{ cm}^2 \text{ V}^{-1} \text{ s}^{-1}$ can be achieved via the introduction of a liquid crystal character to semiconducting polymers;^[10] or by exploiting the self-assembling properties observed in highly regioregular P3HT samples whose polymer chains generate ordered structures (lamellae) normal to the

[*] Prof. I. D. W. Samuel, Dr. S. Gambino, S. G. Stevenson
Organic Semiconductor Centre
SUPA, Department of Physics and Astronomy
University of St Andrews, St Andrews
Fife, KY16 9SS (UK)
E-mail: idws@st-andrews.ac.uk
Dr. K. A. Knights
Chemistry Research Laboratory, Department of Chemistry
University of Oxford, Mansfield Rd, Oxford, OX1 3TA (UK)
Prof. P. L. Burn
Centre for Organic Photonics & Electronics
University of Queensland
School of Molecular and Microbial Sciences
Chemistry Building
Queensland, 4072 (Australia)

DOI: 10.1002/adfm.200801144

substrate and π - π interactions parallel to the plane.^[11] In this latter case the high mobility values were explained by the ability of the polymer to adopt a well-ordered lamellar structure, which enables good transport of charges along the polymers (intrachain transport) as well as between polymer chains in the direction parallel to the substrate. These values drastically drop by more than two orders of magnitude when charge transport is measured in the direction normal to the substrate instead of parallel to the plane.^[12,13] This is a concern because some important optoelectronic devices, namely OLEDs and solar cells require charge transport in the perpendicular direction, so more isotropic materials would be useful for some applications.

Conjugated dendrimers consist of a core, conjugated dendrons, and surface groups.^[14] The dendrons control interactions between the cores, and such interactions can be controlled by the number of levels of branching (generation number) of the dendrimer and/or the number of dendrons attached to the core. This can lead to a more spherical shape and so offers the prospect of more isotropic charge transport. In previous studies of light-emitting dendrimers, charge transport occurred by hopping between the electroactive cores, and higher generation materials had more favorable photophysical properties, but reduced charge mobility.^[15–18] These characteristics have been used to create a family of phosphorescent dendrimers that have given rise to highly efficient OLEDs. The phosphorescent dendrimers have been comprised of iridium(III) complex cores, biphenyl-based dendrons, and 2-ethylhexyloxy surface groups.^[19–21] A particularly effective way of controlling interactions between the cores of these dendrimers has been to increase the number of dendrons close to the core, making so called “double dendron” materials, which have two dendrons per ligand of the core. This has enabled very efficient photoluminescence and electroluminescence to be obtained from neat films,^[22] though again the biphenyl dendrons simply acted as spacers separating the cores, rather than participating directly in charge transport.

In this paper, we explore the charge transporting properties of a family of conjugated dendrimers designed to have improved charge-transport by incorporating carbazole units into the dendrons. We explore the effect of both the generation number and the number of dendrons per ligand on the charge transport, in order to identify the best strategy for enhancing charge transport.

Like polymers, light-emitting dendrimers readily form uniform amorphous thin films by spin-coating from solution. In contrast to polymers they are mono-disperse. The absence of polydispersity removes one of the main causes of energetic disorder. In this work partially and fully encapsulated light-emitting dendrimers with structurally rigid carbazole moieties in the dendrons are shown to have very good charge mobilities. The fully encapsulated dendrimer is a hole transporting material giving rise, to the best of our knowledge, to films characterized by the lowest energetic disorder parameter ever reported for any solution processed material, that is, the narrowest energetic distribution of hopping sites. The best material gives films with time-of-flight (TOF) hole mobilities comparable to films of evaporated small molecules,^[23] and amongst the highest reported for solution processed materials (the highest for a solution processed dendrimer film). Furthermore, we report for the first time the existence of a non-dispersive hole photocurrent transient at 77 K for any solution processed material.

Several methods are available for the measurements of carrier drift mobilities, and the results can depend on the technique used. Measurements of charge transport perpendicular to the substrate are required for OLEDs and solar cells, and can best be performed by the TOF technique. Mobilities measured by TOF give a very accurate representation of the bulk mobility of the material, and depending on the TOF method samples of different thicknesses can be used. This is important as it has been reported that mobility values are thickness dependent, especially for low-mobility dispersive materials.^[24,25]

TOF mobility measurements are most commonly made on films a few microns thick to ensure that the excitation light is absorbed in a layer that is thin compared with the total thickness of the film.^[26,27] However, such films are much thicker than those used in OLEDs or solar cells, and are prepared by techniques such as blade-coating, dip-coating, or solution casting, instead of the spin-coating commonly used to make OLEDs and solar cells. Accordingly in the present study we have used a charge generation layer in order to be able to work with much thinner films that can be prepared by spin-coating,^[28] and are therefore comparable in thickness and morphology to films used in OLEDs.

We compare charge transport between three generations (Ir-CarbG1 to Ir-CarbG3) of a family of dendrimers that consist of a *fac*-tris(2-phenylpyridyl)iridium(III) [Ir(ppy)₃] core, carbazole containing dendrons and 9,9-di-*n*-propylfluorenyl surface groups.^[29] In these materials there is one dendron per ligand of the core. We refer to them as “single dendron” materials and their structures are shown in Figure 1(a–c). We also report charge transport in a first generation double dendron dendrimer (Ir-CarbDDG1) that has the same surface groups and dendrons (Fig. 1d).

2. Results and Discussion

2.1. Single Dendron Materials

We first consider the effect of generation on the charge transport. The room temperature hole photocurrent transients plotted on a linear scale from the first to third generations (Ir-CarbG1, Ir-CarbG2, and Ir-CarbG3) of the carbazole family at the same external applied electric field ($E = 1 \times 10^5 \text{ V cm}^{-1}$) are shown in Figure 2a. The transients have been scaled for better comparison. It is clear that all the three photocurrent transients do not show a constant current plateau but there is still a clear inflection point in the double-log plot (Fig. 2b), indicating the arrival of carriers at the ITO electrode, which allows the measurement of a well defined transit time.

For all three generations of dendrimers the measurement of the hole photocurrent transient was repeated at a range of applied fields, from each transient the transit time was extracted from the intersection point of the asymptotes of the double-logarithmic photocurrent versus time plots. Thus using Eq. (5) the mobility was then obtained at each field, and is plotted against the square root of the applied field in Figure 2c. For the three generations of dendrimer under an applied electric field in the range $(7.3\text{--}20) \times 10^4 \text{ V cm}^{-1}$ the mobility values found are $(3\text{--}6) \times 10^{-5} \text{ cm}^2 \text{ V}^{-1} \text{ s}^{-1}$ for Ir-CarbG1; $(4.6\text{--}9) \times 10^{-5} \text{ cm}^2 \text{ V}^{-1} \text{ s}^{-1}$ for Ir-CarbG2; and $(7.3\text{--}12) \times 10^{-5} \text{ cm}^2 \text{ V}^{-1} \text{ s}^{-1}$ for Ir-CarbG3. At low fields, the dendrimers have a nearly field independent mobility up to a field

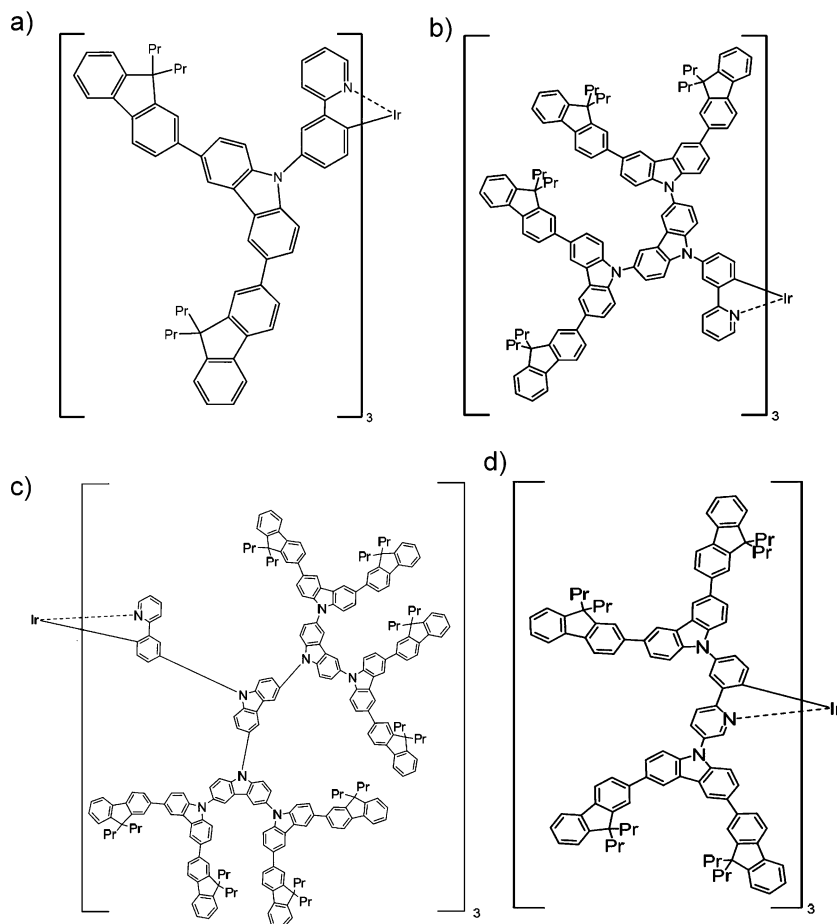


Figure 1. Structures of the carbazole dendrimers: a) Ir-CarbG1, b) Ir-CarbG2, c) Ir-CarbG3, and d) Ir-CarbDDG1-Pr = *n*-Propyl.

of $E = 1 \times 10^5 \text{ V cm}^{-1}$, and then as the field increases further the mobility increases as well showing the so called Poole-Frenkel (PF) behavior:

$$\ln[\mu(E)/\mu_{E=0}] = SE^{1/2} \quad (1)$$

where S is the slope and $\mu_{E=0}$ is the zero-field mobility. Furthermore it can be seen immediately from Figure 2c that as the generation increases the hole mobility also increases. These results are clearly in contrast with previously reported results for other light-emitting dendrimers^[15,17] where on increasing the generation the mobility was lower. This shows that the carbazolyl-based dendrons do not slow the carrier packet by separating the core regions, as reported in the literature for other dendrimers in which charge is hopping between the dendrimer cores.^[15,17] In the present case, the carbazolyl-based dendrons have an active role in charge transport. Molecular orbital calculations have shown that the highest occupied molecular orbital (HOMO) of the dendrimers is delocalized over the core and the carbazole units in the dendrons^[29] enabling charge transport between the carbazole units.

We have been able to investigate the second-generation carbazole dendrimer in more detail because a well defined change of slope between the initial spike and the long tail, depicted as a shoulder, is clearly visible even in the linear plot of Figure 2a. This shape is the remnant of a current plateau resembling non-dispersive charge transport behavior. This allows additional temperature dependent measurements for a complete understanding of the charge transport mechanism. Figure 3a shows the field dependent mobility measurements of this material at temperatures from 235 to 335 K at intervals of 20 K. We analyzed the field and temperature dependent mobility data on the basis of Eq. (2) to determine σ , μ_0 , Σ and C :

$$\begin{aligned} \mu(T, E) &= \mu_0 \exp\left[-\frac{2}{3}\sigma^2\right] \\ &\times \exp\left[C(\sigma^2 - \Sigma^2)E^{1/2}\right] \Sigma \geq 1.5 \\ \mu(T, E) &= \mu_0 \exp\left[-\frac{2}{3}\sigma^2\right] \\ &\times \exp\left[C(\sigma^2 - 2.25)E^{1/2}\right] \Sigma < 1.5 \end{aligned} \quad (2)$$

where σ and Σ are the two central parameters of the disorder formalism; σ the energy width of the hopping site manifold, and Σ is the positional disorder due to a distribution of intersite distances; C is a constant and $\hat{\sigma} = \sigma/kT$. Equation (2) predicts a PF-like electric field dependence for a given temperature. Therefore, we plotted mobility against $E^{1/2}$ at each temperature, as shown in Figure 3a for Ir-CarbG2. Experimental data of Figure 3a

are well described by Eq. (2) for electric field values larger than 10^5 V cm^{-1} [$E^{1/2} > 300 \text{ (V cm}^{-1})^{1/2}$]. This is consistent with the model predicted by Bäessler.^[30]

To understand why the experimental data deviate from Eq. (2) at lower fields we have to take into account both the energetic and the positional disorder parameters.^[30,31] In a hopping system with a spatial distribution of the hopping sites, faster routes as well as dead-ends are created for the carriers executing their random walk. At low fields [$E^{1/2} < 200 \text{ (V cm}^{-1})^{1/2}$], where the heating effect of the field on the energetic distribution of hopping carriers is negligible, increasing the field allows carrier movement but if a carrier reaches a localized or dead end site (such as a site with a poor overlap between adjacent sites) its movement is delayed. The delay arises because any other detour routes made up of more energetically/topologically favorable charge-transporting sites, with part of the path going against the field are forbidden because the field tends to eliminate jumps against the field direction.^[30,32] It is basically this effect that is responsible for the decrease of μ with increasing E . This negative field dependence has been observed in various disordered organic materials.^[32–34] At an electric field range of $200 \leq E^{1/2} \leq 300 \text{ (V cm}^{-1})^{1/2}$ the drift mobility shows a minimum, and within this range the mobility field dependence

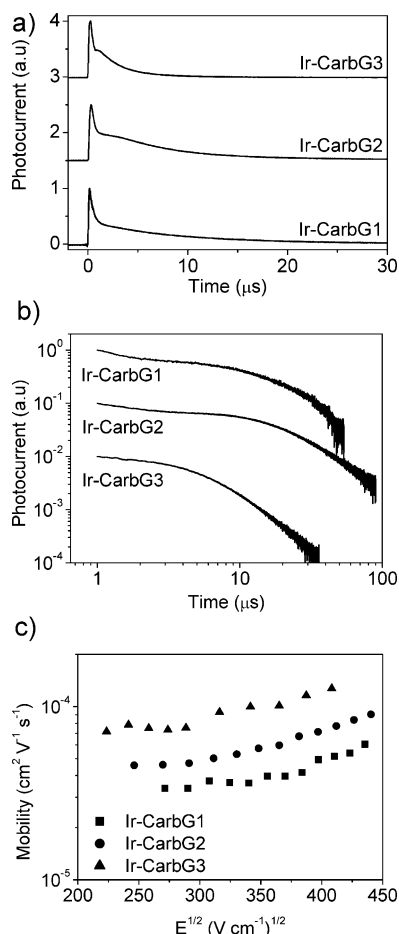


Figure 2. Room temperature Ir-CarbG1, Ir-CarbG2, and Ir-CarbG3 data plots: a) hole photocurrent transients in linear scale for all taken at a field of $1 \times 10^5 \text{ V cm}^{-1}$, b) also shown in double log scale, and c) hole mobility against field.

is very weak. Compared to a previously reported dendrimer [comprised of a bis(9,9-di-*n*-hexylfluorenyl) core, biphenyl-based dendrons, and 2-ethylhexyloxy surface groups (G1-BF)]^[35] the value of the electric field at which mobility reaches a minimum is lower for these dendrimers. This is consistent with a lower value of the positional disorder parameter found in the present work. In this case the influence of the superimposition of the positional disorder on the field dependence of the drift mobility is weaker than in the previously reported dendrimer, which had a positional disorder parameter nearly twice as high.^[35] These results are in very good agreement with Monte Carlo simulations^[32], theoretical,^[36] and experimental^[12] studies recently reported, where with increasing Σ , the low-field behavior tends to bend upward at larger electric field values.

Finally, at larger fields $E^{1/2} > 300 (\text{V cm}^{-1})^{1/2}$ (i.e., $E > 10^5 \text{ V cm}^{-1}$), the faster routes whose direction is not aligned with the direction of the external electric field are diminished, and therefore, the carrier is forced to make the difficult jumps. While this might be expected to give rise to a decreasing mobility with increasing electric field it can be seen in Figure 2c and 3a that the

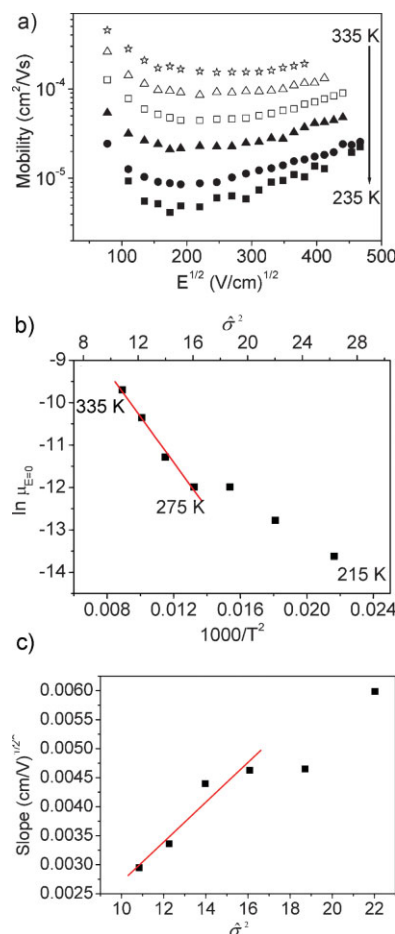


Figure 3. Ir-CarbG2 data plots: a) the field dependent hole mobilities at temperatures from 235 to 335 K at intervals of 20 K, b) zero-field mobilities obtained for the various temperatures against $1/T^2$, c) slope (S) obtained at various temperatures against the value of σ^2 .

mobility increases. The increase in mobility in the present case arises from the fact that there is a strong field effect on the energy barriers along the field direction. It means that at larger fields ($E > 10^5 \text{ V cm}^{-1}$), depending on the magnitude of σ , as a charge carrier hops it is accelerated by the external electric field and gains electrostatic energy equal to qEa (a is the intersite distance, q is the elementary charge), which lowers the activation energy for jumps to higher energy site, and gives rise to the typical PF-like electric field dependence.

The zero-field mobilities obtained for the various temperatures are plotted against $1/T^2$ in Figure 3b for Ir-CarbG2. A linear relationship is observed for $\ln [\mu(0, T)]$ against $1/T^2$ as expected in the Gaussian disorder model (GDM)^[30] from

$$\mu_{(E=0)} = \mu_0 \exp\left(-\left(T_0/T\right)^2\right) \quad (3)$$

where μ_0 is the mobility at infinite temperature and T_0 is the characteristic temperature of the material investigated. From the figure the value of T_0 for Ir-CarbG2 was obtained from the slope as $T_0 = 735 \text{ K}$, and the value of μ_0 from the intercept with

the y-axis as $\mu_0 = 7.3 \times 10^{-3} \text{ cm}^2 \text{ V}^{-1} \text{ s}^{-1}$. The width of the Gaussian density of states (DOS) is related to T_0 through the relation, $T_0 = 2\sigma/3k$, where k is the Boltzmann constant. Hence, given a value of $T_0 = 735 \text{ K}$ for the second generation carbazole dendrimer, the value of width of the density of states was found as, $\sigma = 95 \pm 6 \text{ meV}$.

It can be clearly seen that the experimental data deviate from a straight line at the transition temperature $T_c = 275 \text{ K}$, which is higher compared to the T_c for G1-BF.^[35] The deviation from the straight line in the plot of $\ln[\mu(0,T)]$ versus $1/T^2$ is attributed to the onset of the non-dispersive to dispersive transition.^[30] This means that as the temperature is decreased the photocurrent plateau (i.e., a non-dispersive transient) become less distinct and disappears below temperatures of 275 K. Because this transition is not sharp, at 295 K, which is very close to the transition temperature, the plateau starts to disappear although it can still be seen in Figure 2a. It is noteworthy that $T_c = 275 \text{ K}$ is strikingly close to the value predicted by the GDM (Eq. 4):

$$(\sigma/kT)^2 = 44.8 + 6.7 \log L \quad (4)$$

where L is the thickness of the samples in centimetres. For our film thickness of 330 nm and with a value of σ as determined previously to be 95 meV, according to Eq. (4) the onset of the non-dispersive to dispersive transition should occur at 286 K for Ir-CarbG2, which is similar to that observed experimentally.

The value of Σ was determined by plotting the slope S [determined using Eq. (1)] in the higher field regime ($E > 1 \times 10^5 \text{ V cm}^{-1}$) for various temperatures against δ^2 . The result is shown in Figure 3c for the temperature range 235–335 K, and by fitting the data points for the temperature range 275–335 K, that is within the non-dispersive regime of charge transport,^[30] we extract Σ from the intercept with the x-axis and C from the slope. This analysis yielded a positional disorder parameter of 1.45 and $C = 3.4 \times 10^{-4} (\text{cm V}^{-1})^{1/2}$ for Ir-CarbG2.

2.2. Double Dendron Material

Thus far we have shown that the charge transport can be varied by changing the dendrimer generation. It is also interesting to determine whether increasing the number of dendrons used in the dendrimer structure can also be used to modify the charge transport properties. For this the charge transport in a first generation double dendron iridium(III)-cored carbazole dendrimer (Ir-CarbDDG1) was considered.

The hole photocurrent transient for Ir-CarbDDG1 at 77 K is plotted on a linear scale in Figure 4a. As noted from the figure the shape of the current transient signifies that hole transport is highly non-dispersive even at such a very low temperature (77 K). No transition temperature from non-dispersive to dispersive charge transport was revealed in the temperature range investigated. According to Monte Carlo simulations of the hopping mechanism within a Gaussian DOS a non-dispersive photocurrent transient should be shown for $\delta \leq 3.5$,^[30] which leads for Ir-CarbDDG1 that has its photocurrent transient non-dispersive even at 77 K (see Fig. 4a), to have a width of the DOS of $\sigma \leq 3.5 kT = 20 \text{ meV}$.

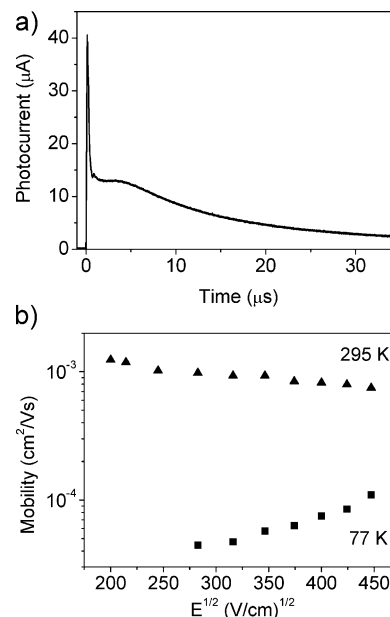


Figure 4. a) Hole photocurrent transient in a linear scale at 77 K for Ir-CarbDDG1, b) field dependent mobility for Ir-CarbDDG1 as a function of the square root of the electric field at temperatures of 295 and 77 K.

The field dependent mobility for Ir-CarbDDG1 is shown in Figure 4b as a function of the square root of the electric field at temperatures of 295 and 77 K. At 295 K the mobility is in the range of $(0.7\text{--}1.2) \times 10^{-3} \text{ cm}^2 \text{ V}^{-1} \text{ s}^{-1}$ whilst at 77 K it has values in the range of $(0.4\text{--}1) \times 10^{-4} \text{ cm}^2 \text{ V}^{-1} \text{ s}^{-1}$. Surprisingly, although the number of levels of branching in Ir-CarbDDG1 is lower than that of Ir-CarbG2 and Ir-CarbG3, the mobility is more than one order of magnitude higher.

The above results for Ir-CarbDDG1, that is, the higher mobility values than Ir-CarbG2 and Ir-CarbG3, together with the highly non-dispersive charge transport behavior at 77 K and the very low width of DOS ($< 20 \text{ meV}$), which to the best of our knowledge is the lowest width of the DOS for a solution processed film ever reported, suggests:

- i) The absence of intrinsic defects, that is, the dendrimer is pure.
- ii) The absence of extrinsic defects, for example, due to oxygen that usually acts as traps for carriers giving rise to a less non-dispersive behavior^[37] or even to a highly dispersive behavior;^[38] or the absence of structural related hole trap states caused by the processing conditions.^[25]
- iii) A better interaction of the electroactive chromophores within the film, which facilitates charge transport. While, it is clear that increasing the number of “conductive” units within the electroactive chromophores in moving from Ir-CarbG1 to Ir-CarbG3 gives rise to an increased mobility, it is less clear why the mobility of Ir-CarbDDG1 is higher. In fact the double dendron dendrimer shows higher mobility values despite having fewer carbazole units within the dendrons compared to the second and third generation single dendron dendrimers. For P3HT it has been shown that the regioregular material shows a better mobility than the regiorandom polymer. For the

dendrimers in this study it seems that in moving from the single to double dendron dendrimers we move from a less ordered film to a more ordered film. The double dendron dendrimer has a greater degree of symmetry due to having dendrons on both (hetero)aromatic units of the ligands of the complex. The improved order is consistent with the lower width of the DOS (<20 meV) compared to single dendron (95 meV). In fact, the disorder formalism is based on the assumption that the distribution of hopping site energies is largely determined by the disorder-induced fluctuation of the electronic polarization energy. Because of the absence of long-range order, hopping sites are located in statistically different environments, thus both hopping site energies and intersite distances are subject to a Gaussian distribution.^[30] We can assume that in a more ordered film during the time a carrier is localized on a hopping site the interaction with the surrounding environment does not differ too much from one site to the next giving rise to a similar polarization energy. This is clearly manifested in smaller variations in the HOMO and LUMO energies and as a consequence gives rise to a narrow distribution of the DOS.

We have also measured the film photoluminescence quantum yield (PLQY) of Ir-CarbDDG1 to be 80%, showing that the improved charge transport is combined with highly efficient phosphorescence. We note that efficient fluorescence and high mobility have recently been reported in a copolymer.^[39]

Furthermore in all the single dendron dendrimers investigated in the present work the room temperature electric field dependence of the mobility at $E > 10^5$ V cm⁻¹ shows a typical $\log \mu \propto SE^{1/2}$ electric field dependence with S being always positive. In contrast, Ir-CarbDDG1 shows a negative field dependence at room temperature, that is, the mobility decreases with increasing field. A room temperature mobility decrease with increasing electric field has been previously observed for several molecularly doped polymer systems,^[33,34,40] for molecular glasses,^[41] and recently for a conjugated polymer,^[42] but never reported for a conjugated dendrimer. Hence, this is the first example of a negative room temperature electric-field dependence of charge carrier drift mobility for a conjugated dendrimer. We argue that the small σ value as well as the presence of the positional disorder is responsible for the negative electric-field dependence of the drift mobility of the Ir-CarbDDG1. This can be understood from the relevant energies. At room temperature the thermal energy (kT) is equal to 26 meV, which is higher than the width of the DOS ($\sigma < 20$ meV). This means that at room temperature charge carriers have enough thermal energy to experience no effective disorder. The charge carriers do not see any energy distribution within the manifold of hopping sites, that is, isoenergetic sites in which the field does not affect intersite jump rates. As a consequence $\mu(E)$ must approach the $\mu \propto E^{-1}$ law expected for a hopping system in which backward transitions are excluded.

3. Conclusions

In summary, we have shown that dendrimers offer a unique opportunity to molecularly engineer materials with high mobilities by changing generation or the number of dendrons. A point to be emphasized is that not only has the introduction of

dendrons with electroactive chromophores improved charge carrier mobility compared to previously reported iridium(III) complex-cored dendrimers, but increasing the number of dendrons strongly affects the charge transport. It is remarkable how in spite of a smaller number of carbazole units in each dendron of the double dendron material, the mobility is more than one order of magnitude higher, because of a less disordered film which facilitates charge transport. The double dendron material has the further advantage of very high film PLQY (80%) so that the improved charge transport is not at the expense of the phosphorescence efficiency. Hence our results show that dendrimers can combine excellent solution processing, charge transporting, and phosphorescence properties.

4. Experimental

For the CGL-TOF measurements, solutions of dendrimer were made to concentrations of 40 mg ml⁻¹ in chloroform. Films were spin-coated onto an ITO substrate at speeds of 700–800 rpm to obtain films around 200–300 nm thick. The samples were then transferred to an evaporator where under high vacuum a 10 nm layer of the absorptive perylene dye (Lumogen Red) followed by 100 nm of aluminum was deposited through a shadow mask to define the active area of approximately 5.6 mm². Testing was undertaken by exciting the charge generation layer through the ITO and dendrimer layer. Charge carriers were generated within the perylene layer by excitation from a 500 ps pulse of a dye laser at a wavelength of 580 nm, which is the peak of the absorption spectrum of Lumogen Red [35]. At this excitation wavelength the dendrimers are completely transparent [43]. The HOMO of the Lumogen Red was estimated from cyclic voltammetry measurements to be 6.2 eV from the vacuum level, enabling hole injection into the dendrimer layer. The packet of charge carriers was then swept through the device under an applied field, and the transit time (t_{tr}) measured using a digital storage oscilloscope. The aluminum electrode was biased positively and the photocurrent signal detected from the ITO. The applied bias led to the electrons photogenerated in the perylene dye layer being removed from the device at the aluminum electrode and holes being injected into the dendrimer from the perylene dye and consequently swept across the device to be collected at the ITO electrode. Thus the measured photocurrent transients are hole currents.

Hole mobilities, μ , were deduced from the transit times, t_{tr} , via the relation

$$\mu = d^2 / V t_{tr}, \quad (5)$$

where d is the film thickness and V is the applied voltage. The sample was mounted in a vacuum cryostat at controlled temperature. The signal to noise ratio is the limiting factor for obtaining data at low temperatures and low applied electric fields. We were able to perform measurements at very low fields and temperatures using a custom made transimpedance amplifier. The RC time constant of the measurement circuit was always selected to be $\leq 20 t_{tr}$. The total charge injected into the film was kept around 2–3% CV in all cases, where C is the capacitance of the device and V the applied voltage. The film PLQY was measured in an integrating sphere under a flowing nitrogen atmosphere following the method of Greenham et al.[44]. The sample was excited by a helium cadmium laser with a wavelength of 325 nm and an excitation power of around 0.2 mW.

Acknowledgements

We are grateful to EPSRC for financial support. Professor Paul Burn is recipient of an Australian Research Council Federation Fellowship (project

number FF0668728). Professor Ifor Samuel is an EPSRC Senior Research Fellow.

Received: April 8, 2008

Published online: December 16, 2008

- [1] Z. Shen, P. E. Burrows, V. Bulovic, S. R. Forrest, M. E. Thompson, *Science* **1997**, 276, 2009.
- [2] C. Taliani, D. D. C. Bradley, D. A. Dos Santos, J. L. Bredas, M. Logdlund, W. R. Salaneck, *Nature* **1999**, 397, 121.
- [3] S. Scheinert, G. Paasch, *Phys. Status Solidi A* **2004**, 201, 1263.
- [4] H. Sirringhaus, *Adv. Mater.* **2005**, 17, 2411.
- [5] J. Nelson, *Curr. Opin. Solid State. Mater.* **2002**, 6, 87.
- [6] H. Hoppe, N. S. Sariciftci, *J. Mater. Res.* **2004**, 19, 1924.
- [7] R. W. I. de Boer, M. E. Gershenson, A. F. Morpurgo, V. Podzorov, in *Physics of Organic Semiconductors* (Ed: W. Brütting), Wiley-VCH, Weinheim, Germany **2005**, Ch. 14.
- [8] N. Karl, *Synth. Met.* **2003**, 133, 649.
- [9] A. Zen, M. Saphiannikova, D. Neher, J. Grenzer, S. Grigorian, U. Pietsch, U. Asawapirom, S. Janietz, U. Scherf, I. Lieberwirth, G. Wegner, *Macromolecules* **2006**, 39, 2162 and ref. therein.
- [10] I. McCulloch, M. Heeney, C. Bailey, K. Genevicius, I. MacDonald, M. Shkunov, D. Sparrowe, S. Tierney, R. Wagner, W. Zhang, M. L. Chabinyc, R. J. Kline, M. D. McGehee, M. F. Toney, *Nat. Mater.* **2006**, 5, 328.
- [11] H. Sirringhaus, P. J. Brown, R. H. Friend, M. M. Nielsen, K. Bechgaard, B. M. W. Langeveld-Voss, A. J. H. Spiering, R. A. J. Janssen, E. W. Meijer, P. Herwig, D. M. De Leeuw, *Nature* **1999**, 401, 685.
- [12] A. J. Mozer, N. S. Sariciftci, A. Pivrikas, R. Österbacka, G. Juška, L. Brassat, H. Bässler, *Phys. Rev. B* **2005**, 71, 035214.
- [13] K. Kaneto, K. Hatae, S. Nagamatsu, W. Takashima, S. S. Pandey, K. Endo, M. Rikukawa, *Jpn J. Appl. Phys.* **1999**, 38, L1188.
- [14] P. L. Burn, S. C. Lo, I. D. W. Samuel, *Adv. Mater.* **2007**, 19, 1675.
- [15] J. M. Lupton, I. D. W. Samuel, R. Bevington, M. J. Frampton, P. L. Burn, H. Bässler, *Phys. Rev. B* **2001**, 63, 155206.
- [16] J. M. Lupton, I. D. W. Samuel, R. Bevington, P. L. Burn, H. Bässler, *Adv. Mater.* **2001**, 13, 258.
- [17] J. P. J. Markham, I. D. W. Samuel, S.-C. Lo, P. L. Burn, M. Weiter, H. Bässler, *J. Appl. Phys.* **2004**, 95, 438.
- [18] J. P. J. Markham, T. D. Anthopoulos, I. D. W. Samuel, G. J. Richards, P. L. Burn, C. Im, H. Bässler, *Appl. Phys. Lett.* **2002**, 81, 3266.
- [19] S.-C. Lo, N. A. H. Male, J. P. J. Markham, S. W. Magennis, P. L. Burn, O. V. Salata, I. D. W. Samuel, *Adv. Mater.* **2002**, 14, 975.
- [20] T. D. Anthopoulos, M. J. Frampton, E. B. Namdas, P. L. Burn, I. D. W. Samuel, *Adv. Mater.* **2004**, 16, 557.
- [21] S.-C. Lo, G. J. Richards, J. P. J. Markham, E. B. Namdas, S. Sharma, P. L. Burn, I. D. W. Samuel, *Adv. Funct. Mater.* **2005**, 15, 1451.
- [22] S.-C. Lo, T. D. Anthopoulos, E. B. Namdas, P. L. Burn, I. D. W. Samuel, *Adv. Mater.* **2005**, 17, 1945.
- [23] H. H. Fong, K. C. Lun, S. K. So, *Chem. Phys. Lett.* **2002**, 353, 407.
- [24] P. M. Borsenberger, L. T. Pautmeier, H. Bässler, *Phys. Rev. B* **1992**, 46, 12145.
- [25] T. Kreouzis, D. Poplavskyy, S. M. Tuladhar, M. Campoy-Quiles, J. Nelson, A. J. Campbell, D. D. C. Bradley, *Phys. Rev. B* **2006**, 73, 235201.
- [26] M. Redecker, D. D. C. Bradley, M. Inbasekaran, E. P. Woo, *Appl. Phys. Lett.* **1998**, 73, 1565.
- [27] A. R. Inigo, H. C. Chiu, W. Fann, Y. S. Huang, U. S. Jeng, T. L. Lin, C. H. Hsu, K. Y. Peng, S. A. Chen, *Phys. Rev. B* **2004**, 69, 075201.
- [28] C. Im, H. Bässler, H. Rost, H. H. Horhold, *J. Chem. Phys.* **2000**, 113, 3802.
- [29] K. A. Knights, S. G. Stevenson, C. P. Shipley, S.-C. Lo, R. E. Harding, S. Gambino, P. L. Burn, I. D. W. Samuel, *J. Mater. Chem.* **2008**, 18, 2121.
- [30] H. Bässler, *Phys. Status Solidi B* **1993**, 175, 15.
- [31] L. Pautmeier, R. Richert, H. Bässler, *Synth. Met.* **1990**, 37, 271.
- [32] P. M. Borsenberger, D. S. Weiss, in *Organic Photoreceptors for Xerography*, Marcel Dekker Inc., New York **1998**.
- [33] A. Peled, L. B. Schein, *Chem. Phys. Lett.* **1988**, 153, 422.
- [34] P. M. Borsenberger, L. Pautmeier, H. Bässler, *J. Chem. Phys.* **1991**, 94, 5447.
- [35] S. Gambino, I. D. W. Samuel, H. Barcena, P. L. Burn, *Org. Electron.* **2008**, 9, 220.
- [36] I. I. Fishchuk, A. Kadashchuk, H. Bässler, M. Abkowitz, *Phys. Rev. B* **2004**, 70, 245212.
- [37] S. Gambino, *PhD Thesis*, Università degli studi di Palermo **2006**.
- [38] G. G. Malliaras, Y. Shen, D. H. Dunlap, H. Murata, Z. H. Kafafi, *Appl. Phys. Lett.* **2001**, 79, 2582.
- [39] B. K. Yap, R. Xia, M. Campoy-Quiles, P. N. Stavrinou, D. D. C. Bradley, *Nat. Mater.* **2008**, 7, 376.
- [40] R. H. Young, *J. Chem. Phys.* **1995**, 103, 6749.
- [41] H. Kageyama, K. Ohnishi, S. Nomura, Y. Shirota, *Chem. Phys. Lett.* **1997**, 277, 137.
- [42] A. J. Mozer, N. S. Sariciftci, *Chem. Phys. Lett.* **2004**, 389, 438.
- [43] S. G. Stevenson, *PhD Thesis*, St Andrews **2008**.
- [44] N. C. Greenham, I. D. W. Samuel, G. R. Hayes, R. T. Phillips, Y. A. R. Kessener, S. C. Moratti, A. B. Holmes, R. H. Friend, *Chem. Phys. Lett.* **1995**, 241, 89.